

The Physics Program of CLAS12

S. Niccolai^a, for the CLAS collaboration

^aInstitut de Physique Nucléaire d'Orsay, Orsay (France)

The experimental program to study nucleon structure at the 12-GeV upgraded JLab using the CLAS12 detector is presented here. The focus of this paper is on deeply virtual exclusive processes, giving access to the Generalized Parton Distributions, and semi-inclusive processes that allow to extract Transverse Momentum Dependent distribution functions. With its wide acceptance, high luminosity, good resolution and particle identification capabilities, large Q^2 and x_B coverage ($1 < Q^2 < 10 \text{ GeV}^2$, $0.1 < x_B < 0.8$), CLAS12 is the ideal facility to pursue the research on the 3-dimensional structure of the nucleon in the valence region.

1. The JLab 12 GeV upgrade and the CLAS12 Detector

The CEBAF (Continuous Electron Beam Facility) accelerator has been delivering up to 6 GeV of high-duty-factor electron beam for hadronic physics research to the three experimental Halls (A, B, and C) of the Jefferson Laboratory (JLab, USA) since 1995. As of today, more than a hundred experiments have been completed, deepening our understanding of the strong interaction and making JLab a world-leading facility in the experimental study of hadronic matter. An energy upgrade of CEBAF to 12 GeV is underway in order to pursue the experimental study of the confinement of quarks (via the search for hybrid mesons) and of the 3-dimensional quark-gluon structure of the nucleons. The CEBAF upgrade to 12 GeV, which will be completed in 2014, will be achieved via 5.5 recirculations through its two existing linacs, in which 10 new high-gradient cryomodules will be added. A new experimental hall, Hall D, devoted to the hybrid mesons studies, will be built, while the capabilities of the detectors in the other three existing halls will be enhanced to suit the new experimental program.

In particular, the Hall-B CLAS12 detector (Fig.1) will be composed of two parts: a Forward Detector (FD) and a Central Detector (CD). The FD will have similar characteristics as the current CLAS [1] but with improved resolution. A toroidal magnetic field will segment the detector

into six azimuthal sectors, each of which will be equipped for identification of charged and neutral particles and tracking. Its acceptance will cover the polar angles between 5° and 40° for charged particles and between 2° and 40° for photons. The CD, equipped for the identification and tracking of backwards-recoiling charged particles, will cover polar angles between 40° and 135° , with full azimuthal coverage. All of its detector components will be housed in a compact superconducting solenoid magnet, which will serve the functions of shielding the tracking detectors from electromagnetic backgrounds and of providing the uniform magnetic field necessary for both the momentum analysis of charged particles at large angles and the operation of a dynamically polarized target.

With its large acceptance, good particle identification capability and high luminosity ($L \sim 10^{35} \text{ cm}^{-2}\text{s}^{-1}$), CLAS12 will be the optimal detector to study nucleon structure at high x_B . Its experimental program for the first 5 years of operation will be based on measurements of:

- Generalized Parton Distributions (GPDs) in exclusive processes,
- Transverse Momentum Dependent (TMDs) distributions in semi-inclusive DIS,
- Parton Distribution Functions in DIS at high x_B ,
- Elastic and resonance form factors,

- Hadronization and color transparency,
- Baryon spectroscopy.

The focus of this paper is on the first two items, GDPs and TMDs studies, which are the core of the CLAS12 experimental program.

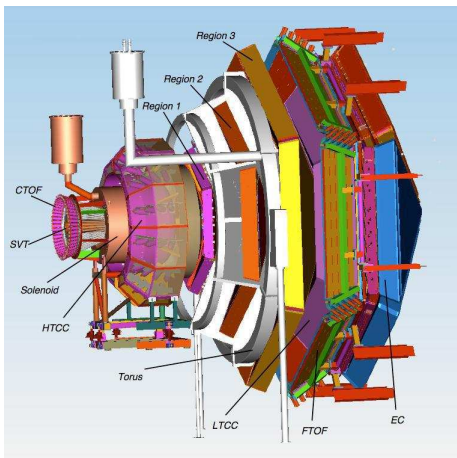


Figure 1. The CLAS12 detector. Its forward part will include: a superconducting toroidal magnet, high- and low-threshold Cerenkov counters (HTCC and LTCC), 3 regions of drift chambers, forward time-of-flight counters (FTOF), electromagnetic calorimeters (EC), and a low-angle inner calorimeter (IC, not visible) for the detection of high-energy photons; the backward part will be composed of a superconducting solenoid magnet containing a silicon vertex tracker (SVT) and time-of-flight counters (CTOF).

2. GDPs in deeply exclusive processes

The Generalized Parton Distributions, introduced nearly a decade ago, have emerged as a universal tool to describe hadrons, and nucleons in particular, in terms of their elementary constituents, the quarks and the gluons [2–6]. The GDPs, which generalize the features of form factors and ordinary parton distributions, describe the correlations between partons

in quantum states of different (or same) helicity, longitudinal momentum, and transverse position. They also can give access, via the Ji’s sum rule [4], to the contribution to the nucleon spin coming from the orbital angular momentum of the quarks. There are four different GDPs for the nucleon: H , E (the two spin-independent GDPs), \tilde{H} , \tilde{E} (the two spin-dependent GDPs), and they can be measured in exclusive hard reactions.

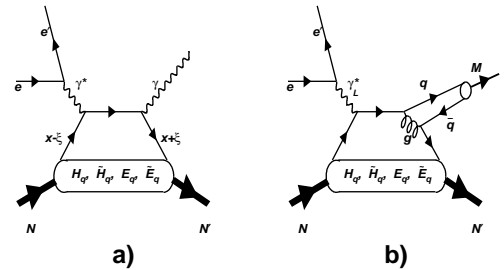


Figure 2. Leading-order “handbag diagram” for DVCS (a) and DVMP (b). x is the average longitudinal momentum fraction of the active quark in the initial and final states, while 2ξ is their difference ($\xi \simeq x_B/(2 - x_B)$, where x_B is the Bjorken scaling variable). The third variable on which the GDPs depend is $t = (p' - p)^2$, the squared four-momentum transferred to the target.

Deeply Virtual Compton scattering (DVCS) on the proton, $ep \rightarrow e'p'\gamma$, is the simplest process to access GDPs. In the Bjorken regime (high γ^* virtuality Q^2 , small squared momentum transferred to the nucleon t) and at leading twist, this mechanism (Fig. 2a) corresponds to the absorption of a virtual photon by a quark carrying the longitudinal momentum fraction $x + \xi$. The struck quark emits a real photon and goes back into the nucleon with the longitudinal momentum fraction $x - \xi$. The amplitude for DVCS is factorized [7] into a hard-scattering part (exactly calculable in pQCD) and a non-perturbative part, representing the soft structure of the nucleon, parametrized by the GDPs, which will depend on the three kinematic variables x , ξ and t . The DVCS amplitude interferes with the amplitude for Bethe-Heitler (BH), the process where the real photon

is emitted either by the incoming or the scattered electron. Although these two reactions are experimentally indistinguishable, the BH is known and exactly calculable via the electromagnetic form factors. Furthermore, their different sensitivity to the polarization of the beam or of the target can also be positively exploited. In fact, the DVCS-BH interference gives rise to spin asymmetries, which can be connected to combinations of GPDs. For instance, the beam-spin asymmetry (BSA), which depends on Q^2 , x_B , t and ϕ (the angle between the leptonic and the hadronic planes), is particularly sensitive to the GPD H , while the contribution of the other GPDs are expected to be negligible [8]. The target-spin asymmetry (TSA), for a longitudinally polarized proton target, can instead give access to a combination of the GPDs H and \tilde{H} . Disposing of a transversely polarized proton target and measuring TSA for DVCS would allow one to extract both H and the less known and constrained GPD E , and therefore be sensitive to the possible different combinations of values for the orbital angular momentum of the quarks. Information about the flavor decomposition of the GPDs via DVCS requires measurements with both proton and neutron targets.

Deeply virtual exclusive meson production (DVMP), Fig. 2b, also allows access to GPDs. By measuring the longitudinal part of the cross section (the factorization hypothesis not being proven for the transverse part) for different mesonic final states one can, as in the case of proton/neutron DVCS, operate a flavor decomposition of the GPDs. Compared to DVCS, however, due to the additional exchange of a gluon, the scaling regime for DVMP is expected to be reached at higher Q^2 .

As of today, the results of pioneering DVCS-dedicated experiments performed at JLab (polarized and unpolarized cross sections in Hall A [9], BSA [10] – Fig. 3 – and TSA with longitudinally polarized target [11] in Hall B with CLAS) suggest that the handbag mechanism dominates already at relatively low Q^2 ($\sim 2 \text{ GeV}^2$). On the other hand, cross section measurements for DVMP (for ρ^0 [12], ω [13], and π^0 [14]) obtained with CLAS at 6 GeV hint that either the scaling

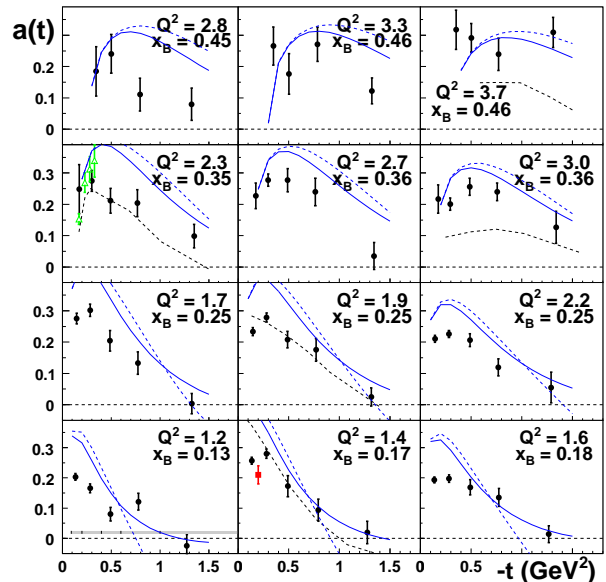


Figure 3. t dependence of the $\sin\phi$ amplitude of the DVCS beam-spin asymmetry, for different $Q^2 - x_B$ bins, extracted from CLAS data at 6 GeV [10]. The blue curves are GPD model predictions [8], the black curves are Regge-based model calculations [15].

regime cannot be reached for values of Q^2 as low as for DVCS or that something is otherwise missing in the existing GPD parametrizations [12].

More data are needed for both DVCS and DVMP:

- at a higher Q^2 , to verify the scaling for DVCS on a wider range, and to approach the handbag regime for DVMP;
- on a wide x_B ($\simeq \xi$) coverage;
- with high accuracy on measured observables to test models (this requires high luminosity);
- performing measurements of various kinds of spin asymmetries (beam, longitudinal and transverse target) and of cross sections.

The CLAS12 setup will fulfill these requirements, providing unprecedented capabilities for exploring nucleon structure via the measurement of GPDs in the valence quark region.

Figure 4 shows the projections for the DVCS BSA that will be obtained running CLAS12 for 2000 hours on a proton target at its nominal ($10^{35} \text{ cm}^{-2}\text{s}^{-1}$) luminosity. The statistical precision of the data and their wide kinematical coverage will put strong constraints on GPD parametrizations. Measurements of unpolarized and polarized DVCS cross sections, as well as TSA and DSA with longitudinally polarized target are also planned [16]. R&D studies are currently underway for the construction of a transversely polarized target for CLAS12, which will allow the extraction of transverse-target single-spin asymmetries (Fig. 5), observables particularly sensitive to the values of the orbital angular momentum of the quarks. Work on the conception of a neutron detector for the CD is also ongoing. It will be necessary to ensure exclusivity in the measurement of DVCS on the neutron – a key reaction to constrain the GPD E .

3. TMDs and semi-inclusive DIS

The present knowledge of the spin structure of the nucleon comes mainly from polarized deeply inelastic scattering (DIS), which is only sensitive to the squared charges of the partons. Semi-inclusive deep inelastic scattering (SIDIS), which requires the detection of a hadron in coincidence with the scattered lepton allowing “flavor tagging”, gives a more direct access to the contributions from the various quarks. It also provides information on the transverse momentum distributions of the quarks, which is not accessible in DIS. The interaction between the active parton in the produced hadron and the spectators leads to the Transverse Momentum Dependent (TMDs) distributions functions, which describe (Table 1) the transition of a nucleon with one polarization in the initial state to a quark with another polarization in the final state [17–19]. TMDs are connected to the orbital angular momentum in the nucleon wave function. TMDs and GPDs are both derived from the same “parent” Wigner distribution - the former obtained via integration on the position of the parton, the latter on its transverse momentum - and thus give complementary information, both contributing to define

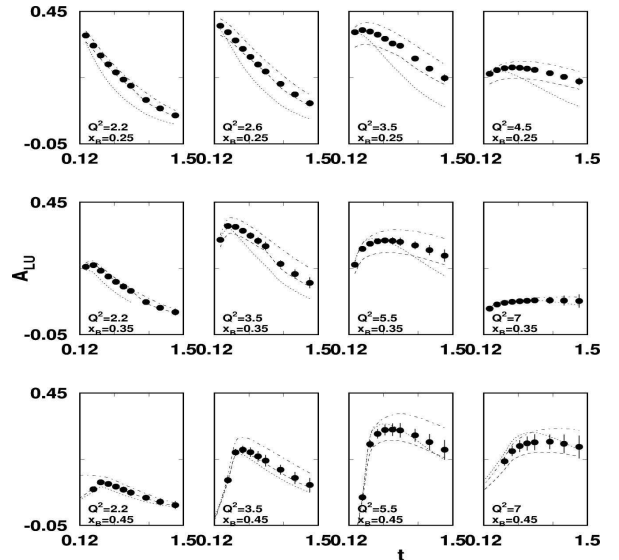


Figure 4. *Expected statistical accuracy for the $\sin \phi$ term of the DVCS BSA, obtainable with CLAS12 after 2000 hours of beam time on a proton target, as a function of t , for the various Q^2 and x_B bins that the CLAS12 acceptance will access. The precision of the data will distinguish among different GPD parametrizations (represented by the curves [8]).*

a 3-dimensional image of the nucleon. The measurement of single- and double-spin asymmetries (SSAs and DSAs) in SIDIS – for different mesonic final states – with transversely and longitudinally polarized targets is necessary for the extraction of the various TMDs for each quark flavor.

The JLab 12-GeV upgrade and the CLAS12 detector will provide the unique combination of wide kinematic coverage, good particle identification, high beam intensity, energy and polarization, which are necessary to study the transverse momentum and spin correlations of quarks via semi inclusive DIS in the valence region. Several experiments are planned, some using the standard CLAS12 configuration and some others requiring additional equipment. The construction of the transversely polarized target (Section 2) will allow the measurements of transverse

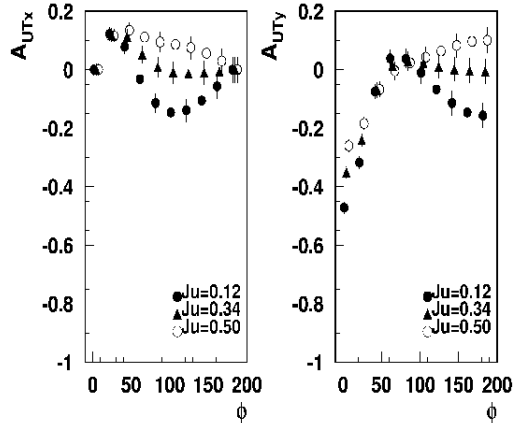


Figure 5. Projected results for the ϕ dependence (for $Q^2 = 2.2 \text{ GeV}^2$, $x_B = 0.25$, $-t = 0.5 \text{ GeV}^2$) of the target-spin asymmetries for a transversely polarized target, for 2000 hours of running with CLAS12. The three kinds of points correspond to different combinations of values for the angular momentum of the u quark.

spin asymmetries – linked to the Sivers and the transversity functions – covering a wider x range than the existing HERMES data [20]. The addition of RICH detectors – another proposed upgrade to the baseline design of CLAS12, which is under study – will extend the study of TMDs to strange quarks, via the measurement of SIDIS with kaons in the final state.

Measurements of transverse momenta of final-state hadrons in SIDIS with longitudinally polarized target will provide information complementary to the ones obtained with a transverse target, probing the longitudinal nucleon structure beyond the collinear approximation [21]. Detailed measurements of the double-spin asymmetry A_{LL} and its $\cos \phi$ moment as a function of P_T (Fig. 7) for different bins in x , z , Q , combined with measurements of azimuthal moments of the unpolarized cross section also proposed for CLAS12, [22] will allow study of the flavor dependence of the transverse momentum distributions.

The $\sin 2\phi$ term of the SSA for longitudinally polarized target gives access to the Kotzinian-Mulders function (h_{1L}^\perp) which measures the mo-

N/q	U	L	T
U	f_1		h_1^\perp (Boer-Mulders)
L		g_1	h_{1L}^\perp (Mulders)
T	f_{1T}^\perp Sivers	g_{1T}	$h_1 h_{1T}^\perp$ (transversity)

Table 1

Leading-twist TMD functions. U , L , and T stand, respectively, for transitions of unpolarized, longitudinally polarized and transversely polarized nucleons (rows) to corresponding quarks (columns).

mentum distribution of transversely polarized quarks in the longitudinally polarized nucleon. A recent measurement of this observable from HERMES [23] at low x_B is consistent with zero (Fig. 6). A large asymmetry has been predicted [24] only at $x_B > 0.2$. The current CLAS data (Fig. 6) [25] have uncertainties too large to draw any conclusion. The CLAS12 data will have the necessary accuracy and coverage.

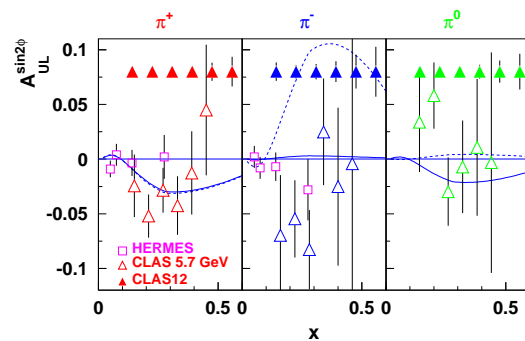


Figure 6. Expected accuracy for the x dependence of the $\sin 2\phi$ term of the target SSA for a longitudinally polarized target, for CLAS12 (full triangles), for π^+ , π^- , and π^0 . The data points come from HERMES [23] (open squares) and CLAS at 6 GeV [25] (open triangles). The curves are model predictions [24].

The double polarization asymmetry A_{LL} for a longitudinally polarized target, connected to the

g_1 function, is sensitive to the difference in the k_T distribution of quarks with spin orientation parallel and anti-parallel to the proton spin. The existing CLAS data [26] for this observable (Fig. 7) don't have the necessary accuracy and P_T coverage to allow discrimination among the various model predictions. The data that will be taken with CLAS12 will have the required sensitivity and reach much higher values of P_T (Fig. 7).

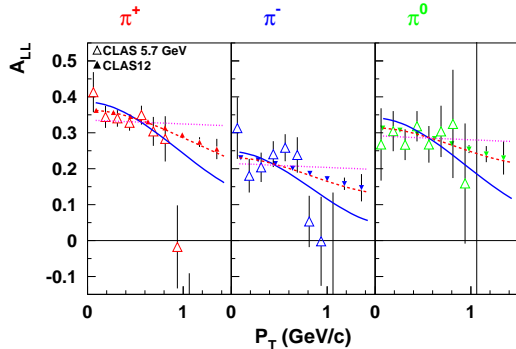


Figure 7. The $\cos\phi$ moment of the double spin asymmetry A_{LL} for longitudinally polarized target as a function of the transverse momentum of the detected hadrons (π^+ , π^- , π^0). The empty triangles are existing CLAS data taken with the 6-GeV beam. The full triangles are projections for CLAS12. The curves are fits by Anselmino *et al.* [27].

4. Conclusions

The JLab 12-GeV upgrade will be essential for the study of the structure of the nucleon in 3D in the valence region with high precision, allowing the measurement of deeply virtual exclusive processes (to access GPDs) and semi-inclusive meson production (to extract TMDs) with polarized beam and targets. CLAS12 will be the only full acceptance, general purpose detector for high-luminosity electron scattering experiments, and it will be perfectly suited for the GPD/TMD program. The first 11-GeV electron beam will hit the CLAS12 target at the end of 2014.

REFERENCES

1. B.A. Mecking *et al.*, Nucl. Instr. Meth. **A503**, 513 (2003).
2. D. Muller *et al.*, Fortschr. Phys. **42**, 101 (1994).
3. A.V. Radyushkin, Phys. Rev. D **56**, 5524 (1997).
4. X.-D. Ji, Phys. Rev. Lett. **78**, 610 (1997).
5. M. Burkardt, Phys. Rev. D **62**, 071503 (2000).
6. M. Diehl, Eur. Phys. J. C **25**, 223 (2002).
7. X.-D. Ji and J. Osborne, Phys. Rev. D **58**, 094018 (1998).
8. M. Guidal, M.V. Polyakov, and M. Vanderhaeghen, Phys. Rev. D **72**, 054013 (2005).
9. C. Munoz Camacho *et al.*, Phys. Rev. Lett. **97**, 262002 (2006).
10. F.X. Girod *et al.*, Phys. Rev. Lett. **100**, 162002 (2008).
11. S. Chen *et al.*, Phys. Rev. Lett. **97**, 072002 (2006).
12. S.A. Morrow *et al.*, Eur. Phys. J. **A39**, 5 (2009).
13. L. Morand *et al.*, Eur. Phys. J **A24**, 445 (2005).
14. I. Bedlinsky *et al.*, analysis underway.
15. J.M. Laget, arXiv:0708.1250 hep-ph (2007).
16. F. Sabatie *et al.*, JLab Proposal E12-06-119.
17. S.J. Brodsky, D.S. Hwang, and I. Schmidt, Phys. Lett. **B530**, 99 (2002).
18. J.C. Collins, Phys. Lett. **B536**, 43 (2002).
19. A.V. Belitsky, X. Ji, and F. Yuan, Nucl. Phys. B **656**, 165 (2003).
20. A. Airapetian *et al.*, Phys. Rev. Lett. **84**, 4047 (2000).
21. H. Avakian *et al.*, JLab Proposal E12-07-107.
22. H. Avakian *et al.*, JLab Proposal E12-06-112.
23. A. Airapetian *et al.*, Phys. Rev. Lett. **B562**, 562 (2003).
24. D. V. Efremov *et al.*, J. Phys. **55**, 189 (2005).
25. H. Avakian *et al.* Phys. Rev **D69**, 112004 (2004).
26. H. Avakian *et al.*, arXiv:1003.4549 hep-ex (2010).
27. M. Anselmino *et al.*, Phys. Rev. **D74**, 074015 (2006).